External Thermal Management Concept for BEV fast charging

Marcus Auch, Timo Kuthada, Andreas Wagner

Institute of Automotive Engineering – University of Stuttgart
Pfaffenwaldring 12
70569 Stuttgart
marcus.auch@ifs.uni-stuttgart.de
timo.kuthada@fkfs.de
andreas.wagner@ifs.uni-stuttgart.de

Abstract: This study investigates the feasibility, conceptualization and thermal modeling of an external thermal management concept for battery electric vehicle (BEV) extreme fast charging (XFC) scenarios. Since BEV standard operating conditions are normally much less challenging from a thermal point of view compared to XFC an external thermal management system has been developed being able to remove the generated waste heat in the XFC process of the BEV. The system consists of an external cooling circuit including a thermal energy storage tank and an external refrigeration circuit removing the waste heat to the environment. The feasibility of the proposed concept has been shown by a developed 1D-simulation of the whole external thermal management concept, delivering insights into additional heat to be removed and sizing of the thermal energy storage tank, pumps, compressors and heat exchangers.

1 Introduction

With the ongoing demand of customers to recharge in a similar timeframe as internal combustion engine vehicles, extreme fast charging (XFC) is one of the most important research topics for battery electric vehicles (BEVs). While the maximum charging power depends on the maximum allowable continuous current applied of the individual cell, it also can be limited due to thermal safety reasons. Depending on the active cathode material used, an operating temperature range of 25 - 40 °C is desired [1]. If the temperature is further increased, there is a risk of thermal runaway of the LIB cell. Thermal runaway is an uncontrolled exothermic reaction inside the LIB cell resulting in big heat releases through the developing gases [2]. If one cell enters the state of thermal runaway there is the risk of thermal propagation, which can result in the explosion of the battery pack and dangerous lithium fires. To prevent those thermal safety issues adequate and reliable thermal management systems are of great importance for BEVs.

For most BEVs, XFC is the most challenging scenario from a thermal point of view. This can be seen by analysing the heat generation occurring inside a LIB. The heat generation in LIBs is dependent on the internal resistance and resulting voltage drop of the LIB cell. The heat generation can be calculated through the simplified Bernardi equation [3]

$$Q_{\text{loss}} = I\,(U_{\text{OCV}} - U_{\text{t}}) - I\,T\,\frac{\partial\,U_{\text{OCV}}}{\partial\,T} \tag{1}$$

whereas U_{OCV} is the LIB open circuit voltage, U_{t} is the LIB terminal voltage, I is the applied current, T is the temperature and $\partial\,U_{\text{OCV}}/\,\partial\,T$ is the entropic coefficient of the LIB cell. Replacing the voltage drop from the open circuit voltage to the terminal voltage with the product of the current I and the internal resistance $R_{\text{i,cell}}$ of the LIB

$$U_{\text{OCV}} - U_{\text{t}} = R_{\text{i,cell}}\,I \tag{2}$$

and then substituting this term into equation (1)

$$Q_{\text{loss}} = I^2\,R_{\text{i,cell}} - I\,T\,\frac{\partial\,U_{\text{OCV}}}{\partial\,T} \tag{3}$$

shows that the first term of the heat generation is proportional to the square of the applied current. While the internal cell resistance is not entirely ohmic resistance, the ohmic resistance share of the total heat generation increases with increasing current applied to the cell. This makes XFC an extremely challenging task for a BEV thermal management system. The maximum temperature must not be exceeded throughout the XFC cycle despite the battery experiencing currents four or eight times higher than those typically applied in the standard driving cycles of the BEV. The aim of the CoolEV project is to explore the potential application of an external thermal management system for XFC of BEVs, with the goal of minimizing the size of the in-vehicle thermal management system to regular operating conditions. The CoolEV consortium consists of Dr. Ing. h.c. F. Porsche AG, Hydac Cooling Gmbh, University of Esslingen, the Zentrum für Sonnenenergie- und Wasserstoff-Forschung Baden-Württemberg (ZSW) and the University of Stuttgart, all contributing to the results of this study.

2 Fundamentals of 1D thermal modeling

The following section presents the fundamentals of modeling cooling circuit and refrigeration components. Furthermore, additional heat inputs by the required cooling circuit components are discussed.

2.1 Modeling of Cooling Circuits

In this study, the cooling circuit modeling approaches for a heat exchanger, a pump, pressure losses due to cooling circuit components and a thermal energy storage tank are necessary. To model heat exchangers, there are several methods available in 1D simulation tools. In this study two different methods are used. An experimental data-based effectiveness-number of transfer units method is utilized for a liquid to liquid heat exchanger and a macroscopic geometrical data method is used for a liquid to refrigerant fluid heat exchanger (also known as chiller). A thermal-hydraulic centrifugal pump is chosen to model the cooling circuit pump. Therefore, the pressure increase

$$\Delta p = f(\dot{m}, w, T) \tag{4}$$

as a function of mass flow rate $\dot{m}$, pump rotation speed w and temperature T can be calculated. Furthermore, an efficiency table also depending on the mentioned parameters

$$\eta_{\mathrm{pump}} = f(\dot{m}, w, T) \tag{5}$$

can be provided to include the losses of the chosen pump. To model the pressure losses occurring inside the cooling circuit two different approaches are used. A simple pipe pressure loss estimation of

$$\Delta p_{\mathrm{pipe}} = f(d_{\mathrm{pipe}}, l_{\mathrm{pipe}}) \tag{6}$$

depending on the diameter d_{pipe} and length l_{pipe} of the pipe can be taken. When experimental data of the pressure loss is available, an experimental based model approach can be used as

$$\Delta p_{\mathrm{coupling}} = f(\dot{m}, T) \tag{7}$$

at specific temperatures and mass flow rates. Lastly, thermal energy storage tanks can be modeled by a thermal-hydraulic capacity model. In this case, the tank requires an initial pressure and temperature as well as the total tank volume V_{tank}. Furthermore, it is possible to include a heat transfer rate to the environment, considering heat losses of the chosen thermal energy storage tank. [4]

2.2 Modeling of Refrigeration Circuits

Refrigeration circuits are mostly vapor compression cycles [5]. One important aspect of vapor compression cycles is the saturation curve of the chosen fluid, which connects the evaporation/condensation saturation temperature with a saturation pressure. This means that additional or removed heat at this specific temperature and pressure will result in a phase change and not an increased or decreased temperature. Using a phase change in cooling systems results in significantly higher moved heats compared to liquid only cooling cycles through the evaporation enthalpy of the chosen fluid [6].

Figure 1 shows the most common refrigeration cycle architectures used. Both architectures consist of the same five components. These are an evaporator (heat exchanger (chiller)), a compressor, a condenser (heat exchanger), an expansion valve and an accumulator. Depending on the position of the accumulator the cycle definition can change.

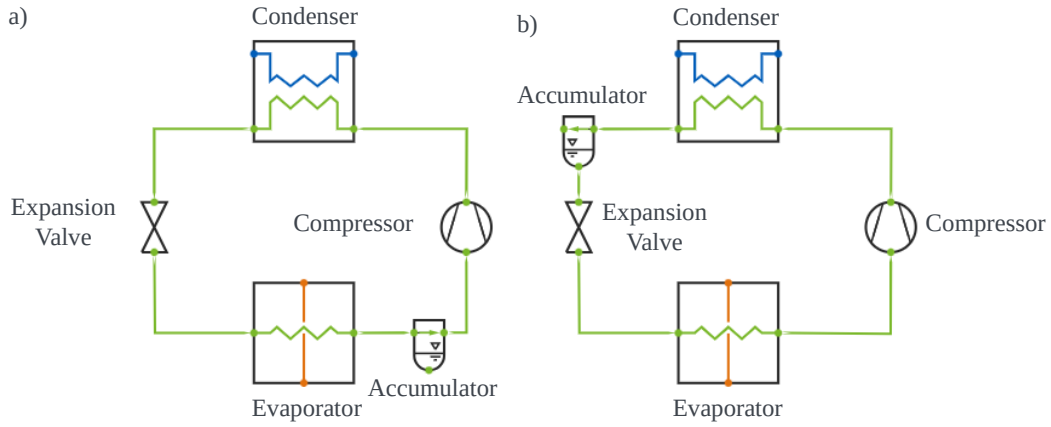

Figure 1: Refrigeration Cycle Designs when integrating an accumulator.
a) Accumulator sets superheat = 0 K, b) Accumulator sets subcooling = 0 K. [7]

However, the overall refrigeration cycle works the same for both architectures. Starting at the evaporator, the fluid enters in liquid (or mixed liquid and gas state) and evaporates completely at low pressure and low temperature while absorbing heat. Then, the resulting vapor is compressed isentropically inside the compressor to a higher pressure and temperature. The compressed vapor (high pressure and temperature) enters the condenser, where it condenses back to liquid while removing heat. The heat removed is the sum of the heat absorbed at the evaporator plus the added energy from the compressor. Lastly, the expansion valve expands the liquid fluid back to low pressure and temperature. The accumulator's function is to control the superheat after the evaporator (Figure 1 a)) or the subcooling after the condenser (Figure 1 b)), depending on the positioning inside the circuit. Both positions can define the thermodynamic cycle.

For the design of refrigeration cycles, the degrees of freedom are the compressor speed, the compressor efficiency, the expansion valve opening, the size of the evaporator and the size of the condenser. These degrees of freedom can be set by the determination of the unknowns, which consist of the evaporation pressure, the condensation pressure, the superheat before the compressor, the temperature after the compressor, the subcooling after the condenser and lastly, the mass flow rate of the refrigerant. While the first five unknown define the thermodynamic cycle, changing the mass flow rate scales the absorbed and removed heat. [7]

The evaporator is modeled by providing the simulation tool the geometrical parameters of a brazed plate heat exchanger. In the CoolEV project the evaporator can be designed by using the Kaori software [8]. The refrigeration compressor pressure increase can be modeled by

$$\Delta p = f(\dot{m}, w, T) \tag{8}$$

with the same parameters as the cooling circuit pump [4]. Furthermore, the isentropic and mechanical efficiency can be calculated with the pressure increase and rotating speed of the compressor

$$\eta_{\mathrm{is,me,compressor}} = f(\Delta p, w) \tag{9}$$

improving the ideal to a real refrigeration cycle. As mechanical efficiency a standard value of 0.99 can be used, while the isentropic efficiency can be calculated depending on the chosen refrigerant fluid [9].

The condenser in this study is modeled with its exact geometrical data. The 1D-simulation software AMESIM then calculates the heat transferred according to the mass flow rates of refrigerant and air with the documented Nusselt-correlations for a microchannel heat exchanger [4]. In the CoolEV project the condenser design software Climetal [10] has been used.

Accumulators are defined by their size and their initial percentage of liquid volume. Depending on the refrigerant chosen and total mass of the refrigerant, an adequate accumulator can be iteratively sized. The sizing should be done to ensure proper accumulator function but not unnecessarily increase the total refrigerant mass. In this study a thermostatic expansion valve is used to control the mass flow rate of the refrigeration cycle depending on the desired superheat after the evaporator.

2.3 Additional Heat inputs

In general, occurring losses result in additional heat inputs into the cooling circuit. Additional heat inputs caused by the pump can be calculated by

$$\dot{Q}_{\mathrm{pump}} = \left(1 - \eta_{\mathrm{pump}}\right) P_{\mathrm{mech}} \tag{10}$$

whereas η_{pump} represents the pump efficiency and P_{mech} the mechanical power of the pump. Additional heat inputs due to pressure losses are calculated by

$$\dot{Q}_{\Delta p} = \Delta p \, \dot{V} \tag{11}$$

whereas Δp is the total pressure loss inside the circuit and $\dot{V}$ represents the volume flow rate in the circuit.

3 Methodology

This chapter presents the conceptualization of the external thermal management system to evaluate its feasibility. Additionally, it presents the design process and set boundary conditions.

3.1 Conceptualization of the external Thermal Management System

The concept for the external thermal management is developed in the CoolEV project [9] and shown in Figure 2. In total, there are three different circuits involved, connected by heat exchangers. The first circuit is the vehicle cooling circuit, in which the oil Opticool has been chosen as working fluid. This study assumes the loss behaviour of the LIB pack to be constant over the whole XFC scenario. Therefore, the battery can be presented as a boundary condition of waste heat that needs to be removed from the vehicle cooling circuit, without modeling its internals. However, should it be necessary to model a dynamic loss behaviour of a real LIB pack, it is also possible to implement an additional battery pack model. [9]

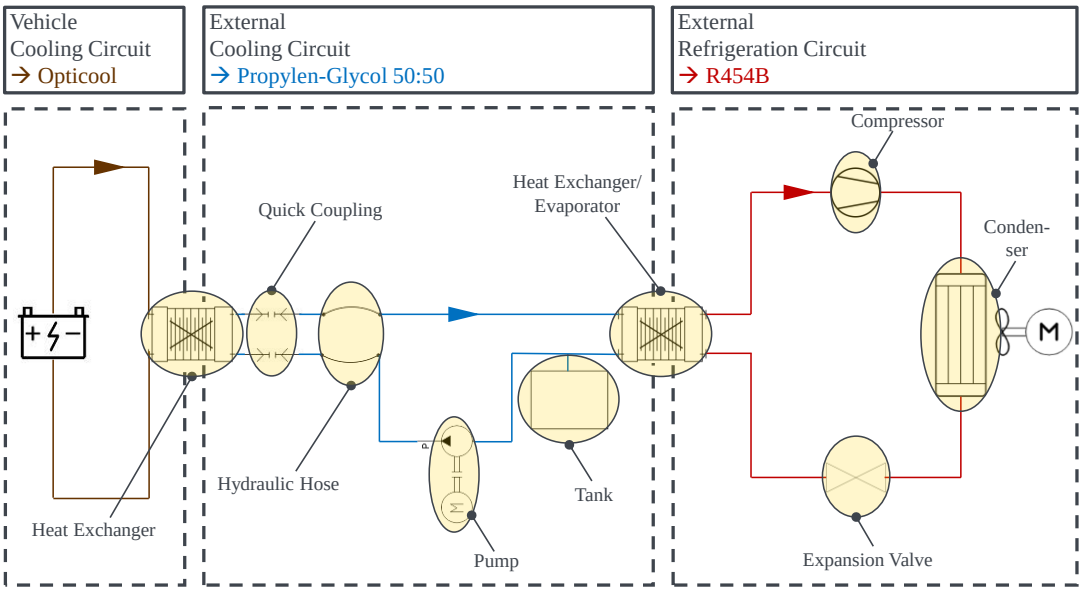

Figure 2: Conceptualization of the external thermal management concept for XFC of BEVs.

The second cycle is the external cooling circuit, running with HYDAC Coolant N50, which is Propylen-Glycol 50:50 (PGL). The external cooling circuit's purpose is to remove the total waste heat of the LIB pack. However, it is not required to

instantaneously remove the total battery waste heat. Therefore, a thermal energy storage tank integration is studied. This would allow to decrease the size of other components (especially in the refrigeration circuit) while still removing all the waste heat over an increased period. Furthermore, a cooling fluid coupling to the vehicle is necessary to connect the vehicle cooling and the external cooling circuit. Therefore, a quick coupling and hydraulic hoses are necessary to allow drivers to easily couple the external cooling system with the vehicle cooling circuit, similar to the electrical coupling systems. Lastly, as in all cooling circuit designs, a pump is needed to fulfill the requirements of the desired volume flow rate. This includes overcoming all pressure losses occurring inside the external cooling circuit. [9]

The last component, the heat exchanger/evaporator, connects the external cooling circuit to an external refrigeration circuit. The refrigeration circuit is responsible for removing the battery pack waste heat to the environment, with R454B as working fluid. Refrigeration circuits use the heat transfer characteristic benefits of phase changes inside the fluid to remove more heat with less power required compared to standard cooling circuits [6]. The refrigeration circuit consists of evaporator, compressor, condenser, accumulator and expansion valve and can be designed by using the thermodynamics fundamentals of a vapor compression cycle.

Figure 3 shows the design process for the external thermal management concept. The design starts with the parameters defined in the CoolEV project [9]. These consist of the inlet heat exchanger oil temperature, the battery waste heat, the oil volume flow rate and the maximum pressure loss allowed of the vehicle cooling circuit. By choosing an adequate heat exchanger that makes the removal of the heat possible, the PGL heat exchanger inlet temperature and the PGL volume flow rate can be determined. Choosing the quick coupling system and hydraulic hose lengths and diameters as well as the heat exchanger pressure losses enables a suitable pump design. The remaining parameters depend on the concept of the thermal energy storage tank. The tank design sets the amount of heat the evaporator must remove, which in turn determines the design of the refrigeration circuit components.

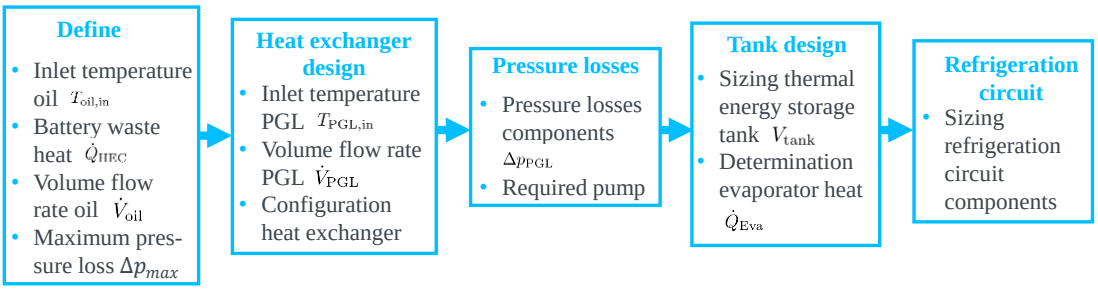

Figure 3: Design process of the external thermal management concept.

In total, four thermal energy storage tank integration concepts are studied and shown in Table 1. In general, the bigger the tank, the smaller the components of the refrigeration circuit can be. However, this benefit comes with a disadvantage of a longer rest time frame after every XFC, during which no other BEV can be charged. The final design is a trade-off between size of the refrigeration circuit, size of the thermal energy storage tank and necessary rest time after every XFC at the charging station.

Table 1: Design options for the thermal energy storage tank.

Concept	**Phase 1: XFC time in min**	**Phase 2: Break time in min**	**Heat Evaporator in kW**	**Heat stored in tank per second in kJ**	**Tank size**
A) No tank	10	0	27.5	0	0
B) Big tank	10	10	13.75	13.75	463
C) Medium tank	10	5	18.33	9.17	309
D) Small tank	10	3	21.1	6.4	215

The tank size can be calculated by taking the density ρ and specific heat capacity c_p of the chosen cooling fluid of the external cooling circuit. In this study, this is PGL, with a freezing point of $\mathrm{T} = -32\,℃$ which enables a safety margin to the minimum temperature design point in the external cooling circuit of -15°C. The tank size is estimated by

$$V_{\mathrm{tank}} = \frac{Qt}{\rho c_{\mathrm{p}} \Delta T} \tag{12}$$

whereas Q represents the heat in J stored per second, t the total storage time and ΔT the maximum temperature increase inside the thermal storage tank. As long as the maximum temperature increase is within 5 K for the studied cooling medium PGL, equation (12) is sufficient to calculate the tank volume. However, for higher temperature increases, the density and specific heat capacity would need to be adapted to the real start and end temperature values of the fluid inside the thermal storage tank.

Additionally, in appendix Figure A.1, the tank temperature (T_{tank}) development of the studied concepts is shown. In the CoolEV project, option B) has been chosen [9]. This option provides a good trade-off between refrigeration circuit component size and maximum rest time. As a result, the external thermal management system is divided into two different phases. One phase is the XFC which takes 10 min and the second phase is the 10 min rest time after every XFC.

3.2 Boundary Conditions

This section will discuss the boundary conditions of the external thermal management system which result from the previously chosen thermal energy storage design. The boundary conditions as well as the built 1D thermal simulation model in Amesim are shown in Figure 4. The boundary conditions of the vehicle cooling circuit can be set according to the XFC. The XFC is defined as a constant battery waste heat loss of 27.5 kW, which has to be removed for 10 min. This represents an XFC from 10 to 80 % State of Charge (SOC) in 10 min. The second boundary condition of the vehicle cooling circuit is the maximum pressure loss resulting of the vehicle cooling circuit pump design. The maximum pressure loss on the vehicle cooling circuit inside the heat exchanger has been set to $\Delta p_{max} = 0.225$ bar resulting in an additional design requirement for the heat exchanger between vehicle and external cooling circuit [9].

To limit the cooling circuit pressure loss to Δp_{max} on the vehicle cooling circuit, a configuration consisting of two heat exchangers have been chosen. This configuration enables to fulfill the pressure loss, inlet temperature of the vehicle circuit and volume flow rate requirements [9]. Therefore, the chosen heat exchanger design determines the external cooling circuit volume flow rate and heat exchanger inlet temperature. In order to remove the required amount of heat a volume flow rate on the external cooling circuit of 50 l/min is necessary with a heat exchanger inlet temperature on the external cooling circuit between -15 °C and -10 °C. The low required inlet temperatures necessitate PGL as the external cooling circuit fluid, because it freezes at lower temperatures than comparable fluids.

The required volume flow rate and the occurring pressure losses define the pump of the external cooling circuit. The pump needs to overcome the combined pressure losses of the heat exchangers, the hydraulic hose and the quick coupling system. The pressure increase and efficiency of the chosen pump are shown in appendix Figure A.2. The data is taken from a centrifugal pump by Grundfos [11]. Therefore, the pressure increase corresponding to the volume flow of the cooling fluid and the efficiency can be directly sourced from the provided data sheets.

The length of the hydraulic hose has been chosen as 5 m to allow the customer to easily plug and unplug the quick coupling system. As quick coupling system a liquid adapter solution by the company Stäubli [12] has been chosen, providing the pressure losses for all external cooling circuit components. The pressure losses depending on the volume flow rate for the chosen quick coupling CGO12 by Stäubli are shown in appendix Figure A.3.

Modeling refrigeration circuits is more complex than modeling cooling circuits. The main difference is the phase. However, several design points need to be fixed before addressing the components. One of the most important aspects is the choice of the refrigeration fluid. The refrigeration fluid needs to have adequate evaporation temperature and pressure to be able to absorb the heat at all desired operation points.

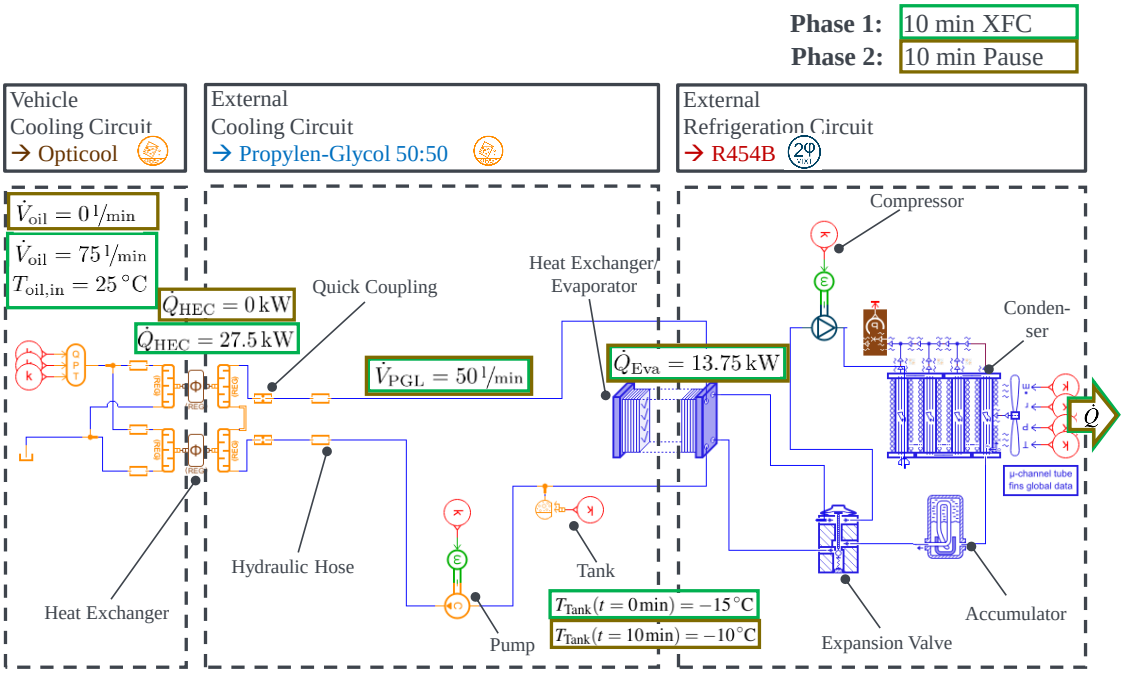

Figure 4: Defined boundary conditions of the external thermal management concept for XFC of BEVs.

The designed refrigeration cycle for the chosen refrigerant fluid R454B is shown in Figure 5 and consists of four steps. First, the vapored fluid is compressed in the compressor, Then, the refrigerant fluid condenses in the condenser until the fluid is at full liquid state. In this study, an accumulator is used after the condenser to ensure a subcooling of 0 K. After the accumulator, the liquid fluid goes through the expansion valve, which adjusts the mass flow rate so that the expanded liquid at lower pressure fully evaporates in the evaporator. If there is no full evaporation of the liquid, the compressor will suffer damage due to liquid ingestion. Therefore, an overheating of 5 K is set to be controlled by the expansion valve mass flow control unit. This guarantees full evaporation in all design points and dynamic profiles.

The refrigeration cycle design starts with the chosen refrigerant fluid R454B. Next, the evaporation and condensation temperature need to be determined. The evaporation process requires lower refrigerant temperatures than the external cooling circuit, while the condensation process requires higher refrigerant temperatures than the ambient temperature. Since the minimum cooling fluid temperature is −15 °C, the evaporation temperature has been set to −16 °C. Furthermore, the maximum ambient temperature defined in the project CoolEV is $T_{amb} = 30$ °C. To ensure a safe operation and limited condenser size, the condensation temperature has been set to 47 °C. The pressure levels of the refrigeration cycle are determined by the saturation curve of R454B, being p_{Eva} = 4.22 bar and p_{Con} = 26 bar. Lastly, the chosen compressor must be able to compress the refrigerant to the desired pressure, which is an isentropic compression process.

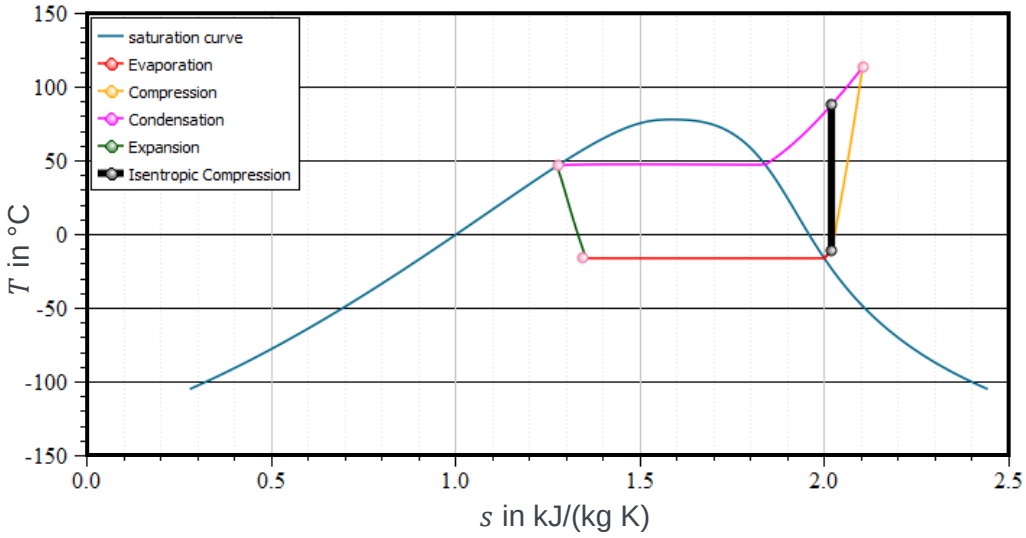

Figure 5: Wet steam region of the refrigerant R454B including the design points of the vapor compression cycle in a T-s diagram. [4]

The values for the compressor can be calculcated from the desired evaporation heat, the evaporation and condensation temperatures as well as the refrigerant fluid. A software tool by Bitzer [13] has been used for an adequate compressor design. The resulting necessary condensation heat and mass flow rate are shown in appendix Figure A.4. The expansion valve design is an iterative process, especially when using a thermostatic expansion valve, which controls the mass flow rate according to the desired superheat of the vapor after the evaporator. The heat transferred during all four processes are shown in Table 2 for the Bitzer design as well as for the 1D thermodynamic cycle in AMESIM. This results in a Coefficient of Performance (COP) of the refrigeration cycle of $\mathrm{COP} = Q_{\mathrm{Con}}/P_{\mathrm{Compressor}} = 2.84$.

Table 2: Powers of desinged vapor compression cycle processes in Amesim and Bitzer software.

	Transformation	**Power Amesim in kW**	**Power Bitzer in kW**
1	Evaporation	15.1	15.5
2	Compression	8.3	8.5
3	Condensation	23.6	24
4	Expansion	0.2	-
5	Mass flow rate in kg/h	313	314

4 Results

In total, three XFC/Pause cycles have been simulated resulting in a total simulated physical time of $t = 3600$ s with a simulation time step of $\Delta t = 2$ s. Additional heat inputs in the external cooling circuit have been considered, resulting in adjusted boundary conditions for the refrigeration circuit. The results of the heat exchangers and thermal energy storage tank temperature are presented to demonstrate the system's ability to meet the demands of the external thermal management system.

4.1 Heat exchanger Vehicle cooling circuit

Figure 6 shows the heat transferred over the first $Q_{\mathrm{HEC},1}$, second, $Q_{\mathrm{HEC},2}$, the sum of both $Q_{\mathrm{HEC,sum}}$ and the mean heat over all three XFC cycles $Q_{\mathrm{HEC,sum,mean}}$. While in the first XFC cycle the heat transferred differs by 10 % between Heat exchanger 1 (HEC1) and HEC2 for the second and third XFC, the removed heat is the same over both HECs. Hence, the temperature difference between external cooling circuit and vehicle cooling circuit is high enough, so that the higher inlet temperature of HEC2 compared to HEC1 does not influence the heat transfer. Additionally, during the rest time Phase 2, no heat is transferred between the vehicle and external cooling circuit. The average transferred heat in the XFC cycles is at $Q_{\mathrm{HEC,sum,mean}}$ = 27.56 kW, fulfilling the cooling requirements of the LIB pack during XFC of 27.5 kW.

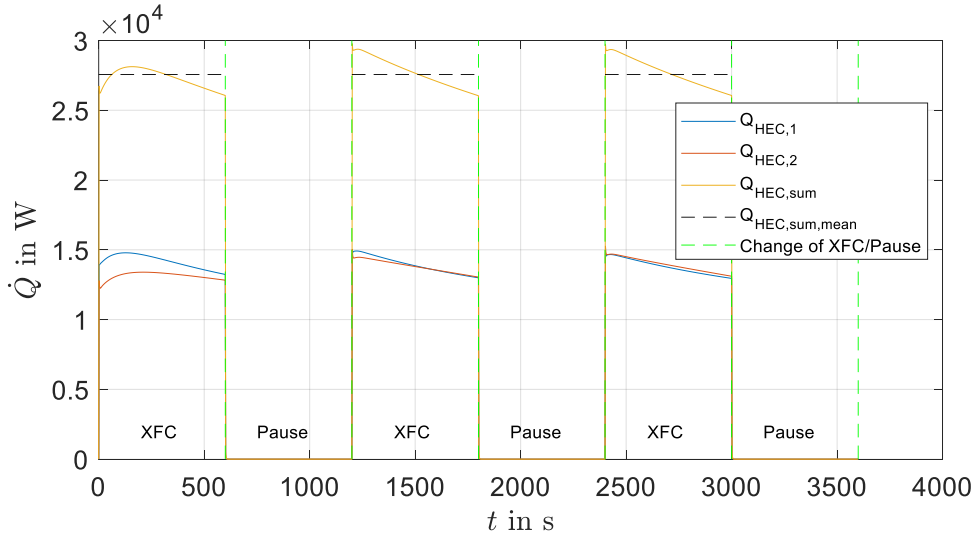

Figure 6: Heat transferred over three XFC/Pause cycles through both heat exchangers between vehicle and external cooling circuit.

4.2 Additional heat input

The simulation model reveals an additional heat input from the external cooling circuit. The additional heat input results from the combined effect of the pump efficiency and the pressure losses. By using equations (10) and (11), the additional heat inputs can be calculated. The external cooling circuit pump has an almost constant efficiency of $\eta_{\mathrm{pump}} = 0.269$ and a mechanical power of $P_{\mathrm{mech}} = 1.33$ kW. This equals an additional heat input due to the pump of $\dot{Q}_{\mathrm{pump}} = 0.97$ kW. A pressure loss of $\Delta p = 4.23$ bar inside the external cooling circuit results from the simulation. At a volume flow rate of $\dot{\mathrm{V}} = 50$ l/min this equals an additional heat input due to the pressure losses of $\dot{Q}_{\Delta p} = 0.35$ kW. Hence, the combined additional heat inputs, which need to be removed in both concept phases equal to 1.32 kW increasing the heat to be removed through the evaporator by 10 % to $\dot{Q}_{\mathrm{eva}} = 15.07$ kW. Therefore, the additional heat needs to be considered in the conceptualization of the refrigeration circuit.

4.3 Evaporator heat

The evaporator has been designed to remove $\dot{Q}_{\mathrm{eva}} = 15.07$ kW in average over the XFC/pause cycle. However, in the design process a constant removed heat over the evaporator has been assumed. This is not true for the real dynamic behavior of the external thermal management design. The reason is the changing boundary conditions of the vehicle and external cooling circuit.

Due to the XFC/pause design, the removed heat over the same evaporator cannot be kept constant. The external cooling circuit's evaporator inlet temperature changes depending on wheter it is in an XFC or pause phase. During XFC there is a large amount of battery waste heat (27.5 kW) delivered into the external cooling circuit. This increases the external cooling circuit fluid temperature and hence, the inlet temperature at the evaporator on the liquid side. Higher inlet temperatures result in higher temperature differences between external cooling fluid and refrigerant and hence, a higher heat transfer. However, during the pause phase, there is no heat delivered into the external cooling circuit. Therefore, the evaporator inlet temperature is lower in the pause phase compared to the XFC phase. To still be able to remove the constant heat of 15.07 kW over both cycles, a larger compressor is necessary. The larger compressor increases the heat transfer during XFC and thus, can compensate for the decreased heat transfer in the pause phase. This also influences the necessary thermal energy storage tank sizing. The final evaporation heat removal results can be seen in Figure 7. The average removed heat over the evaporator over three XFC/Pause cycles results in $\dot{Q}_{\mathrm{Eva,mean}} = 15.2\ kW$ and therefore, fulfills the requirement of removing 15.07 kW heat. However, the larger compressor decreases the COP of the refrigeration circuit.

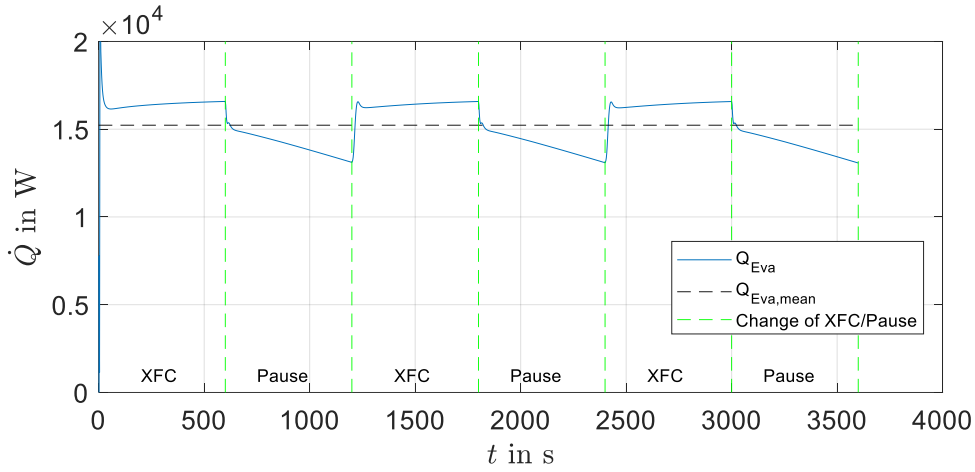

Figure 7: Heat transferred over three XFC/Pause cycles through the evaporator.

4.4 Condenser heat

The results for the heat removed to the environment by the condenser are shown in Figure 8. The higher the ambient temperature the more challenging the task is for the condenser, because the temperature difference between refrigerant fluid and environmental air decreases. Therefore, an ambient temperature of $T_{\mathrm{amb}} = 30$ °C has been chosen for the simulation to ensure operation over all environmental conditions. Because of the increased compressor size and the resulting increased losses, more heat must be removed by the condenser than designed. The chosen condenser is suitable for the increased heat loads and does not need to be replaced. The condenser heat follows the same trend as the evaporator heat regarding the XFC and pause phases. On average, the condenser removes $\dot{Q}_{\mathrm{Con,mean}} = 27.3$ kW and fulfills the requirements of the conceptualization.

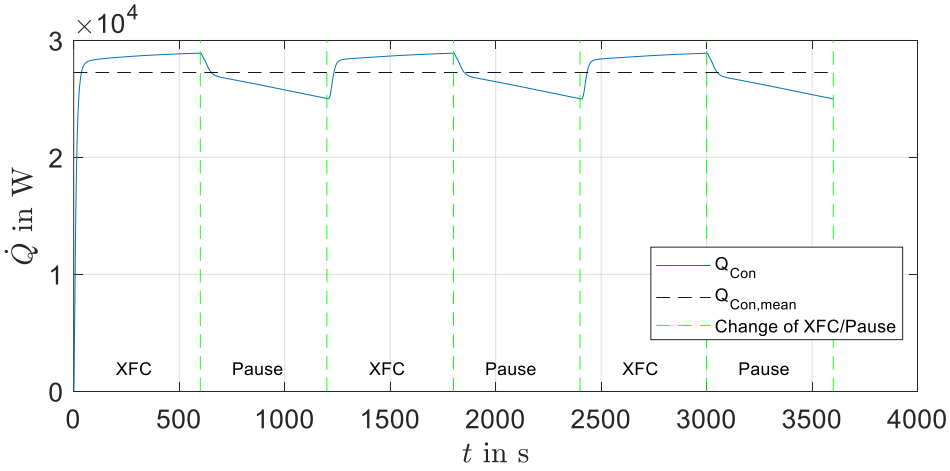

Figure 8: Heat transferred over three XFC/Pause cycles through the condenser to the environment.

4.5 Tank sizing

To determine the inital boundary conditions, the tank has been dimensioned with a simple heat balance equation (12) involving the start and end temperatures desired in the tank as well as the time frames for XFC and pause. However, the total system simulation is influenced by dynamic modeling and changing inlet temperatures at the evaporator. The enlarged compressor and hence, increased heat removal during the XFC phase allows a downsizing of the tank. This can be done iteratively after the refrigeration and external cooling circuit parameters are set. Compared to the initial calculated value of 463 l the tank can be decreased by 40 l (approx 10%) to 420 l. An additional effect allowing a smaller tank is that some of the liquid cooling fluid is spread out in the heat exchanger and pipes. The tank temperature over time over three XFC/pause cycles is shown in Figure 9. The set limits of an inlet temperature between -15 °C and -10 °C for the vehicle to external cooling circuit heat exchangers can be fulfilled.

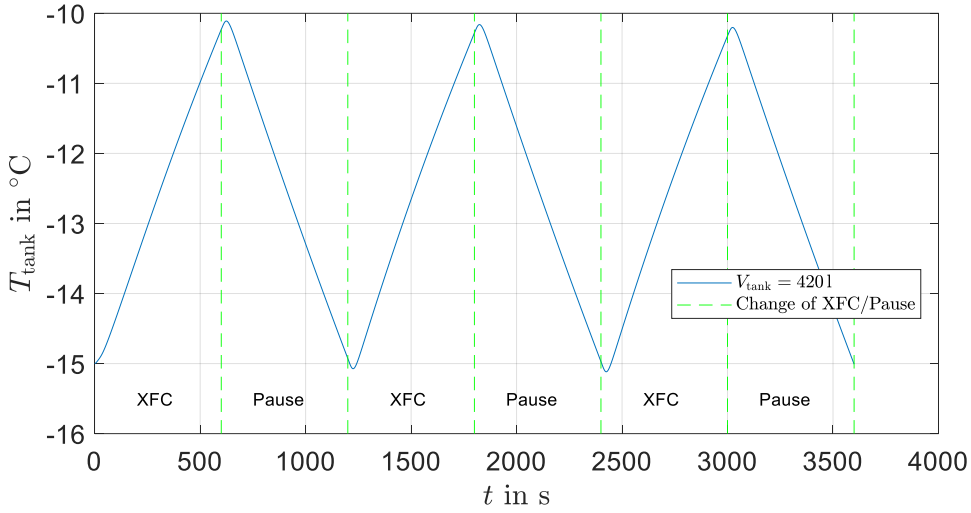

Figure 9: Tank temperature over three XFC/Pause cycles in the thermal energy storage tank of the external cooling circuit.

5 Conclusion

In this study, an external thermal management system for XFC scenarios of BEVs has been designed . The conceptualization and design process is presented. Furthermore, the boundary conditions set to fulfill the requirements for the removed heat are shown. In the 1D-simulation tool AMESIM, a simulation framework has been built, being able to model the external thermal management concept. The results have shown the feasibility of the designed system for the application of external thermal management systems in XFCs.

The developed simulation framework can further be used for sensivity and optimization studies. With changing heats to be removed or specifications of the cooling fluids inside the circuits, all other components can be scaled to fulfill new requirements for different BEV architectures and cells. However, this study uses a maximum heat to be removed scenario to be able to work for most BEV XFC cases. By developing an adequate control system, which could be a PID control between the desired vehicle cooling circuit heat exchanger outlet temperature and the condenser fan rotation speed (mass flow rate of the air) the developed concept should be suitable to all common BEVs.

6 Acknowledgments

This research is accomplished within the project “CoolEV”. We acknowledge the financial support for the project by the German Federal Ministry of Economic Affairs and Climate Action (BMWK) as part of the "Electric Mobility" funding program.

7 Bibliography

[1] Pesaran, Ahmad A. "Battery thermal models for hybrid vehicle simulations." Journal of power sources 110.2 (2002): 377-382.

[2] Feng, Xuning, et al. "Thermal runaway mechanism of lithium ion battery for electric vehicles: A review." Energy storage materials 10 (2018): 246-267.

[3] Bernardi, D., E. Pawlikowski, and John Newman. "A general energy balance for battery systems." Journal of the electrochemical society 132.1 (1985): 5.

[4] Siemens, "Simcenter Amesim User Manual." (2023).

[5] Sumeru, K., H. Nasution, and F. N. Ani. "A review on two-phase ejector as an expansion device in vapor compression refrigeration cycle." Renewable and Sustainable Energy Reviews 16.7 (2012): 4927-4937.

[6] Németh-Csóka, Mihály. Thermisches Management elektrischer Maschinen. Springer: Wiesbaden, Germany, 2018.

[7] Gräber, M., “Why receivers and accumulators in refrigeration cycles?” (2020) Accessed on 01/09/2023, url: https://tlk-energy.de/blog/warum-gibt-es-sammler-und-abscheider-im-kaeltekreislauf

[8] Kaori Heat Treatment Co., LTD., Accessed on 01/09/2023, url: https://www.kaori.com.tw/en/modules/nc_product/

[9] CoolEV Consortium, “Design and project requirements of the external thermal management system by the CoolEV consortium” (2022).

[10] Climetal, S.L., “Climetal Microchannel Simulation”, Accessed on 10/07/2023, url: http://webapp.climetal.com/Account/Login.aspx?ReturnUrl=%2f

[11] Grundfos GMBH, “MTH 4-6/6 A-W-A-AQQV”, Accessed on 01/09/2023, url: https://product-selection.grundfos.com/de/products/mt-tank-mounted-pumps/mth/mth-4-66-98993064?tab=variant-curves&pumpsystemid=2157052039

[12] Stäubli International AG, Accessed on 01/09/2023, url: https://www.staubli.com/de/de/corp.html

[13] Bitzer Kühlmaschinenbau GmbH, “Bitzer Software 6.18.0”, Accessed on 01/09/2023, url: https://www.bitzer.de/de/de/tools-archiv/software/software/versionen -software.jsp

8 Appendix

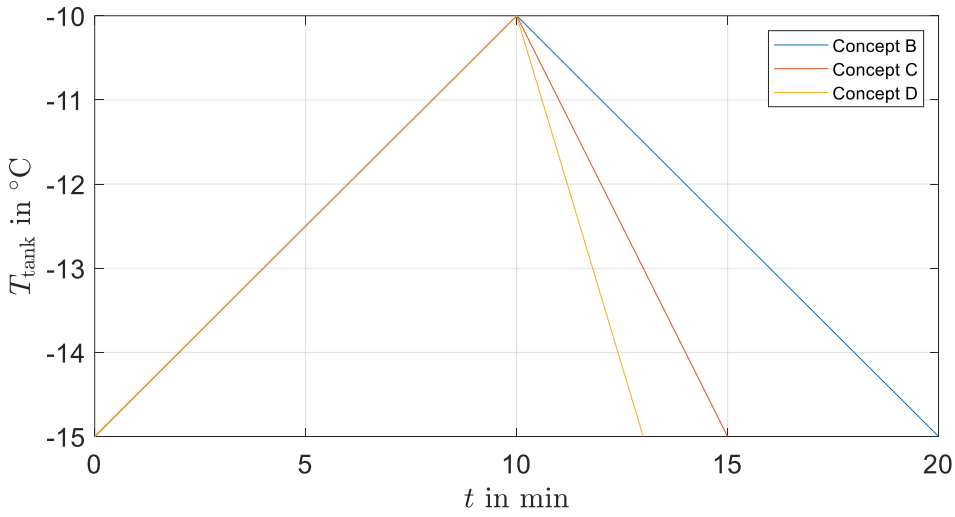

Figure A.1: Tank temperature development for three different thermal energy storage tank concepts.

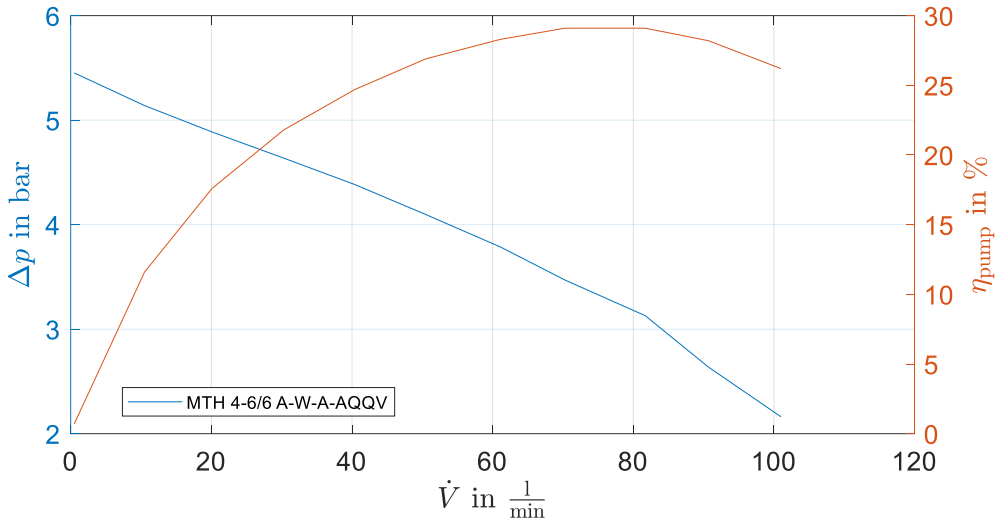

Figure A.2: Pressure increase and efficiency dependent on the volume flow rate for the chosen cooling pump by Grundfos [11].

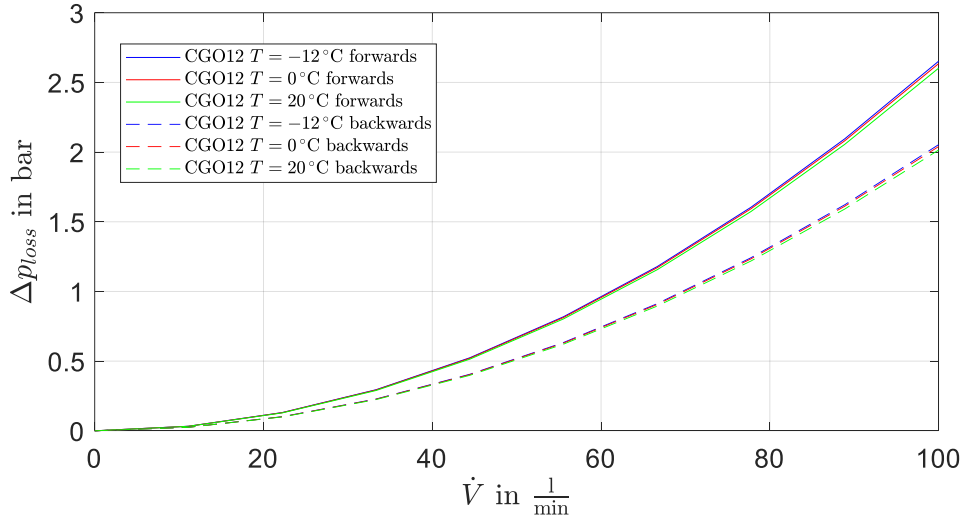

Figure A.3: Pressure losses of the chosen quick coupling configuration CGO12 by Stäubli [12]. Distinguished between forward and backward flow direction.

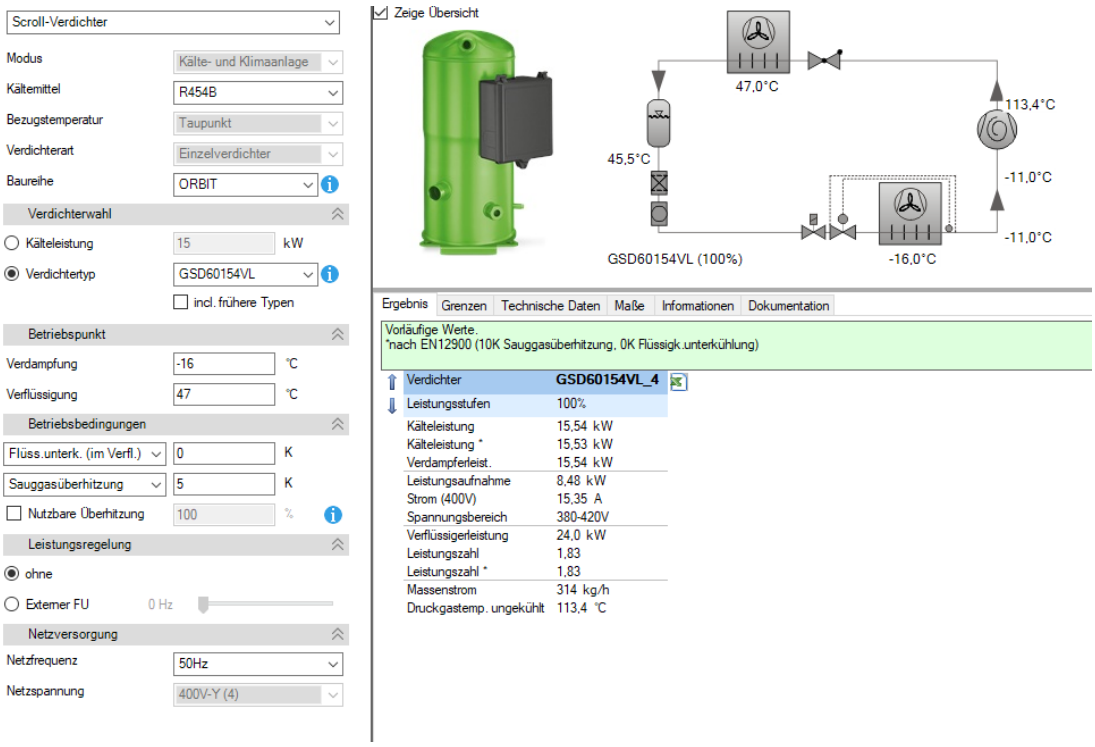

Figure A.4: Bitzer data of the designed compressor. [13]